ELSEVIER

Cold Regions Science and Technology 35 (2002) 123–145

cold regions science and technology

www.elsevier.com/locate/coldregions

A physical SNOWPACK model for the Swiss avalanche warning Part I: numerical model

Perry Bartelt, Michael Lehning *

WSL, Swiss Federal Institute for Snow and Avalanche Research, SLF, Flüelastrasse 11, CH-7260 Davos Dorf, Switzerland

Abstract

The numerical formulation of a one-dimensional physical snowpack model is presented. The model is operationally employed on a day-to-day basis by avalanche warners to predict snowpack settlement, layering, surface energy exchange and mass balance. Meteorological data obtained from automatic weather stations positioned near avalanche starting zones is used as model input. In this paper, the one-dimensional equations governing the heat transfer, water transport, vapour diffusion and mechanical deformation of a phase changing snowpack are stated. New snow, wind drift and snow ablation are treated as special mass boundary conditions. Snow is modelled as a three-component (ice, water, air) porous material capable of undergoing large irreversible viscous deformations. Phase changes between the components are simulated. Snow layers are defined not only in terms of height and density, but also microstructure. That is, by the size, shape and bonding of the grains composing the ice lattice. The governing differential equations are solved using a fully implicit Lagrangian Gauss–Seidel finite-element method. Example calculations from the catastrophic avalanche winter 1999 are presented to document model performance. The overall mass balance evaluation shows that the model accurately predicts the build-up and ablation of the seasonal alpine snowcover.

Keywords: Snow; Heat and mass transfer; Snow deformation; Phase change; Finite element model; Avalanche

1. Introduction

An extreme avalanche period overcame Switzerland on February 1999. During this intense 1-month period, over 3000 avalanches occurred; 1000 of these caused damage to residential areas, agricultural land and power and transportation lines. Avalanche fracture heights of over 5 m were observed, indicating avalanche return periods of well over 100 years (SFISAR, 2000). A total of 17 people were killed, 12 alone in Evolène Canton Wallis.

Although tragic enough, the damage could have been greater had not a new avalanche warning system been in operation. An integral part of this warning system is the numerical modelling of the snowpack in order to augment information obtained from direct human observations and a large network of fully automated weather stations (Lehning et al., 1999). The model provides avalanche forecasters with supplementary information in cases where digging snowpits is impossible (bad weather), too time-consuming or simply too dangerous.

The purpose of this paper is to describe the snowpack model (called SNOWPACK), which numerically solves the partial differential equations governing the mass, energy and momentum conservation within the

* Corresponding author. Tel.: +41-81-417-0158; fax: +41-81-417-0110.

E-mail address: lehning@slf.ch (M. Lehning).

0165-232X/02/$ - see front matter
PII: S0165-232X(02)00074-5

snowpack using the finite-element method. The numerical model has been constructed to handle the special problems of avalanche warning.

1. Since most avalanches occur during or after periods of intense snowfall, special numerical procedures have been introduced to treat new snowfall. These procedures add finite elements to the existing snowpack mesh. To model snowdrift finite elements can also be added or subtracted from the existing finite-element grid. This requires a highly dynamic program data structure. Furthermore, special algorithms are required to determine the initial physical properties (density, microstructure, temperature) of the new and drifted snow.

2. For avalanche forecasters, the rate of snowpack settling provides important insight into the mechanical stability of the snowcover. The race between increasing strength, i.e. density, and applied load must be modelled. To determine the densification rate, snow is treated as a viscoelastic material capable of undergoing large, instationary deformations. The kinematic description allows for large irreversible, volumetric strains.

3. The model is presently used in ''now-casting'' mode: meteorological data is retrieved from the weather stations and then used to drive the numerical model. SNOWPACK can simulate the snowcover for several hours, days, weeks, months or even years. For avalanche forecasters, however, the short-term (several hours) development of the snowpack is of interest. This means that calculations must be started and, when no meteorological data is available, stopped. The calculations can then be ''restarted'' as soon as possible. Data from the previous simulations are not lost since it is required for the next calculation.

4. Avalanche forecasters are interested in snowpack layering. Layers are defined by their size as well as their macroscopic and microscopic properties. Macroscopic properties include bulk density, mean stress, water content or temperature. Microscopic properties include ice grain size and shape, bond size or coordination number. Sharp layer discontinuities exist. Forecasters want to know the location of thin weak layers. For this reason, SNOWPACK tracks the microstructural properties of the ice lattice over time using temperature gradient (TG) and equitemperature (ET) metamorphism routines. Constitutive relations such as the creep viscosity, which governs snow settlement, and thermal conductivity, which governs the energy transport within the snowcover, are formulated in terms of both macroscopic and microscopic snow properties and are, therefore, highly nonlinear. It is important to note that in order to track snowpack layers, the numerical model must employ a deforming material coordinate system, a so-called ''Lagrangian'' formulation.

5. The quantitative influence of solar radiation or strong warm winds (Föhn) on the stability of the snowcover is difficult to predict due to the complex energy exchange on the snowpack surface. Determining surface melting and the transport of meltwater through the snowcover is essential for predicting the release of wet snow avalanches. Meltwater refreezes to form thin ice layers. In SNOWPACK, all phase changes are mass and energy conserving. Since snow is modelled as a three-component (ice, water and water vapour) porous material, phase changes between the ice and water phases (surface and subsurface melting, meltwater refreezing) as well as phase changes between the ice and vapour phases (deposition and sublimation to and from the ice lattice) are accounted for.

6. Mass can be removed from the snowpack by wind erosion, meltwater runoff or water vapour sublimation. Since avalanche formation is strongly related to drifting snow, the physical treatment of mass erosion at the snowpack surface is necessary. From the numerical standpoint, this means removing finite elements from the surface, based on some erosion criteria. This information is used to formulate a drift index which is subsequently used by forecasters to predict avalanche hazard. Snow ablation is also predicted in SNOWPACK by removing surface elements which contain only water (the ice phase has completely melted). The water flows downward, heating the snowpack; that is, it refreezes on the subzero ice lattice. In an isothermal snowpack, water reaches the bottom and exits the snowcover.

Snowpack models have been developed for many different snow science and snow engineering applications. Probably the most advanced is the French SAFRAN–CROCUS–MEPRA chain which is used for avalanche warning in France and Switzerland (Brun et al., 1989, 1992). Snowpack models based on the mixture theories of Morland et al. (1990) have been proposed to model snowpack behaviour. These

models are based on the rigid application of Truesdell's theory of mixtures and postulate conservation equations for the ice, water, water vapour and air constituents of the natural snowpack. However, because of the mathematical complexity of this general theory, reduced models have been derived by making simplifying assumptions such as a rigid ice matrix (no settling) (Gray and Morland, 1994), no water content (dry snowpacks) (Gray and Morland, 1995), or no snow metamorphism (Bader and Weilenmann, 1992). We stress that for our operational applications, no such simplifications are allowed. The full complexity of the natural snowpack must be modelled. At the same time, we are in complete agreement with Gray et al. (1995) that snowpack models must rest on a sound theoretical foundation and not ad hoc implementations of snow physics.

In the following, Part I, we first discuss the underlying physical assumptions of the model and the finite-element solution of the governing differential equations, including the numerical treatment of phase changes, new snowfall and snow ablation. We discuss the differences between our model and other existing snowpack models such as the French model (Brun et al., 1989), the mixture theory models of Morland (Morland et al., 1990), the CRREL model (Jordan, 1991) or the earlier SLF model, DAISY (Bader and Weilenmann, 1992). The paper ends with a modelling of the catastrophic avalanche winter 1999 and a detailed mass balance evaluation of the instrumented test site, Weissfluhjoch.

No description of a physical snowpack model is complete without a detailed discussion of its constitutive laws. We have placed this discussion in a separate paper, Part II (Lehning et al., this issue a), in order to emphasize the importance of thermomechanical microstructural constitutive formulations in snowpack modelling. However, since the constitutive laws employed in the model are based on snow microstructure, we first must discuss snow temperature gradient (TG) and equitemperature (ET) snow metamorphism algorithms that predict snow grain and grain bond growth. In Part II, we present our microstructural constitutive laws for snow viscosity and heat conduction. They will not be discussed in this paper.

In a separate and final paper, Part III (Lehning et al., this issue b), we present aspects of the model pertaining to operational avalanche forecasting as well as the results of our extensive validation work. This includes a detailed treatment of the energy exchange at the snowpack surface. The algorithm to determine snow precipitation rates which is required to drive the model—especially in hazardous situations—is also presented. The validation in Part III includes the modelling of thin weak layers and a statistical evaluation of the snow profile simulation.

The present work is, thus, the first part of a snowpack modelling triptych composed of *numerical modelling*, *snow microstructure* and *constitutive modelling* and *operational model evaluation*. The last part contains meteorological boundary conditions and thin-layer formation.

2. Snowpack modelling

Consider Fig. 1 which shows a multilayered snowpack and many of the physical processes we want to model. Let z be the coordinate perpendicular to a slope with angle ϕ; $z=0$ defines the snowpack base and $z=h$ the snowpack surface. At some time t, we are interested in finding the physical properties of the snowpack, for example, the vertical temperature distribution $T_s(z, t)$ or the density of the snowpack layers $P_s(z, t)$. In our one-dimensional model, we assume that all slope parallel velocities (creep movements and water flow) are zero. In addition, all lateral gradients (temperature and vapour pressure) are likewise zero.

Similar to mixture theory, we describe each snow layer using three constituents: ice, water and moist air. Each snow layer is defined by the volumetric fractions, θ_i, θ_w and θ_a ($i=1=$ice, $w=2=$water, $a=3=$moist air). By definition, the volumetric fraction is between 0 and 1 and

$$\theta_i + \theta_w + \theta_a = 1. \tag{1}$$

The above relationship is rigidly enforced for all settling, phase change and mass transport operations. Intrinsic constants are defined per unit constituent volume, for example, ice density, P_i, and are used to define all macroscopic partial variables, i.e.

$$P_s = P_i\theta_i + P_w\theta_w + P_a\theta_a, \tag{2}$$

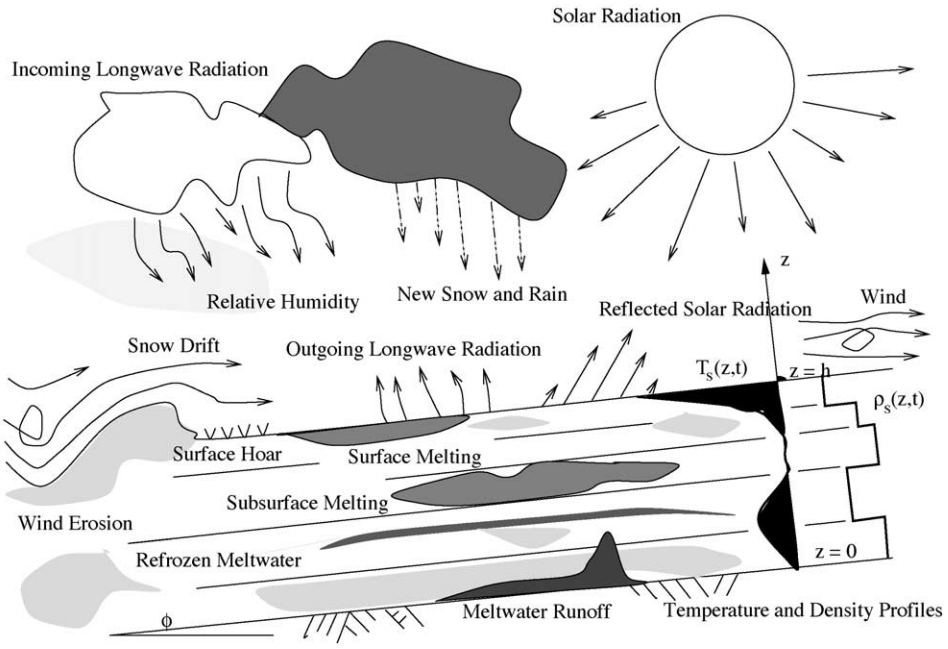

Fig. 1. Important physical processes in snowpack modelling.

where P_s is the snow density, P_w and P_a are the water and moist air densities, respectively.

At any given time t, we assume that the ice, water and moist air constituents have the same common temperature, which we refer to as the snow or bulk temperature, T_s. This assumption is made since the meteorological boundary conditions (short- and long-wave radiation, sensible and latent heat transfers) are defined as bulk energy exchanges at the snowpack surface. To define energy exchanges for each constituent phase (at the snowpack surface or between phases) would be theoretically possible, but would be difficult, if not impossible, to experimentally verify, especially in the field. The automatic weather stations measure a single temperature. Thus, a single bulk energy equation is postulated to determine the vertical temperature distribution, $T_s(z, t)$, within the snowpack. Basically, we assume that the energy exchange between the snow constituents occurs at a much faster rate than the meteorological energy exchange at the snowpack surface. This assumption also reduces the computational demands of the model.

All meltwater phase changes and interlayer water vapour transport processes are subsequently energy and mass conserving. When the ice constituent phase melts ($T_s = 0$ °C, $\theta_i > 0$) or meltwater refreezes ($T_s < 0$ °C, $\theta_w > 0$) energy sink or source terms, respectively, are placed on the right-hand side of the bulk energy equation which are proportional to the constituent mass changes. This process will be described in more detail in Section 6. The energy from the mass changes constrain the temperature field $T_s(z, t)$ to the melting/refreezing $T_s = 0$ °C temperature. A similar procedure is also applied between the ice and moist air phases: water vapour mass is either deposited onto the solid ice phase such that the snow vapour pressure $p_a(z, t)$ is never greater than the fully saturated vapour pressure $p_s(z, t)$. Moreover, we calculate the mass changes (in the form of crystal growth) and energy supply which are required to enforce the pressure constraint, $p_a(z, t) = p_s(z, t)$. The snowpack can be undersaturated and the vapour pressure distribution is governed by the vapour diffusion equation.

We assume that the self-weight of the snowpack is carried entirely by the solid ice lattice. The snow stress, $\sigma_s(z, t)$ is the mean stress which can vary significantly from the microstructural grain-bond stress, $\sigma_b(z, t)$. The air or water surrounding the ice lattice does not directly resist motion. Grain bond strength, however, is directly related to water content,

θ_w, and bulk temperature, T_s. The coordination number and the free space between grains, which is proportional to the air content, θ_a, is also decisive for snow strength (St. Lawrence and Bradley, 1975; Kry, 1975; Gubler, 1978; Hansen and Brown, 1987; Mahajan and Brown, 1993; Bartelt and von Moos, 2000). These considerations lead to the assumption that only a single momentum conservation equation for the solid ice lattice is required. Momentum conservation for the air and water phases is not considered. The influence of air and water on snow deformation is not treated via interconstituent momentum exchanges, as in mixture theory, but rather via constitutive equations for snow elasticity and viscosity. The primary reason for this assumption is that it is much easier to experimentally verify constitutive formulations, for example via triaxial testing than interconstituent momentum transfers.

Mixture theory models, like most fluid dynamic applications, usually employ a Eulerian coordinate system, meaning that the constituents move relative to a stationary computational grid. This approach is not followed. A Lagrangian coordinate system that moves with the ice matrix is employed. There are four important advantages of formulating the ice constituent momentum equation in Lagrangian or material coordinates.

1. If the calculated displacement field is continuous (which it is in the finite-element method), the mass continuity equation of the ice phase is automatically fulfilled. Moreover, in the three-constituent system, only two mass conservation equations are required—one for the water phase and one for the water vapour phase.

2. Since the only requirement in a Lagrangian formulation is displacement field continuity, discontinuities in layer density are possible (one finite element can have another density as an adjacent element). In a Eulerian formulation, the mass conservation equation enforces the continuity of the density field at the solution nodes. This is physically unrealistic.

3. The position of the top snowpack surface is known exactly because it corresponds to a displacing finite-element node. Thus, the treatment of thermal and mass (new snow) boundary conditions is greatly simplified (see Gray and Morland, 1994 for the alternative Eulerian procedure).

4. The history of the material is known. It is impossible to track snow microstructure parameters using a Eulerian formulation since material history is lost. Eulerian based snowpack models cannot be used for the avalanche forecasting since the most relevant information regarding stability—the existence of weak snowpack layers is difficult, if not impossible, to predict.

An important consequence regarding the fourth and final advantage is that it is possible to formulate constitutive laws which are based on snow microstructure. Since all mechanical and thermodynamical properties of the snowpack are a function of snow microstructure (grain and bond size, grain shape, grain history), microstructure-based constitutive equations for both snow viscosity and heat conduction are necessary in order to model real snowpacks. We have found in our investigations that constitutive models which are based solely on continuum parameters (density, temperature, volumetric water content) are inadequate for operational avalanche warning because they cannot accurately model snowpack layering. For example, if nonmicrostructure-based viscosity laws are applied, the calculated density profile increases with depth. This does not agree with snowpit observations where smaller densities can exist in the interior of the snowpack. However, the prerequisite to model this behaviour is that snow microstructure is parameterized and laws exist that describe how these parameters change as a function of temperature and temperature gradient (Part II).

3. Governing differential equations

A strict application of the principles of mass, energy and momentum conservation for each of the constituent phases (ice, water and air) would lead to a system of nine governing differential equations. However, because of our modelling assumptions listed above, only four differential equations are required.

1. All three constituents are assumed to be at the same bulk temperature, $T_s(z, t)$. Heat transport is described by an effective conductivity, $k_e(z, t)$; surface energy exchanges by bulk heat fluxes. One, instead of three, energy equations is, therefore, required.

2. A single-momentum equation governs snowcover settlement since the entire self-weight of the

snowpack is assumed to be carried by the ice lattice. Momentum conservation of the water and air phases is not considered.

3. The equation describing mass conservation of the ice phase is not required because a Lagrangian (or material) coordinate system is employed in the numerical solution of the ice-phase momentum equation. Since the numerical solution for the displacement field, $U_i(z,\ t)$, is continuous, mass conservation of the ice phase is automatically fulfilled. A mass conservation equation for the ice phase is subsequently not necessary.

In summary, snowpack behaviour is described by two mass conservation equations for the vapour and water phases, one bulk temperature equation and one momentum equation for the ice phase, which, because of our choice of coordinate system, automatically fulfills the third mass conservation equation.

We state the equations below. The spatial coordinate, z, is defined normal to the slope surface (see Fig. 1). The symbol, t, represents time. All variables with the subscript s refer to bulk snow quantities. All variables are listed in the Appendix of Part II.

3.1. Bulk temperature equation (energy conservation)

The conservation of energy leads to the following bulk energy equation:

$$P_s(z,\ t)c_s(\theta,\ z,\ t)\frac{\partial T_s(z,\ t)}{\partial t} - k_e(\theta,\ z,\ t)\frac{\partial^2 T_s(z,\ t)}{\partial z^2} = Q_{pc}(z,\ t) + Q_{sw}(z,\ t) + Q_{mm}(z,\ t), \quad (3)$$

where P_s is the snow density and c_s is the specific heat capacity of snow at constant pressure,

$$P_s c_s = P_i c_i \theta_i + P_w c_w \theta_w + P_a c_a \theta_a, \quad (4)$$

k_e is the bulk conductivity, which is usually written as,

$$k_e = k_i \theta_i + k_w \theta_w + k_a \theta_a. \quad (5)$$

In our numerous validation studies, we have found this formulation for k_e to be inferior to empirical or microstructural thermal conductivity models. A detailed discussion of k_e will be presented in Part II. The right-hand side contains Q_{pc}, an energy sink or source term accounting for melting and meltwater refreezing, respectively (Section 6), Q_{sw}, the short-wave radiation energy source term (Part III) and Q_{mm}, a vapour diffusion energy sink or source term (Section 7) representing the latent heat contribution of sublimation and deposition of water vapour on the ice matrix. This effect is usually considered by modifying the thermal conductivity, k_e (Jordan, 1991), especially when assuming that the water vapour does not move. In our current operational version, we take this approach (Part II) while for research purposes, we model instationary water vapour transport directly. This is described in the following paragraph.

3.2. Vapour diffusion equation (mass conservation of air phase)

The pore air is modelled as a binary mixture of dry air and water vapour. The pore air pressure P_a is the sum of the partial pressures of the component parts (Dalton's Law)

$$P_a = P_v + P_d, \quad (6)$$

where P_v is the partial water vapour pressure and P_d is the partial pressure of dry air. Because the vapour and dry air occupy the same volume, a similar relation exists for the air density

$$P_a = P_v + P_d. \quad (7)$$

Assuming that the air is an ideal gas, the relation between densities and pressures are

$$P_v = \frac{p_v \mu_v}{R T_s} \quad (8)$$

and

$$P_d = \frac{p_d \mu_d}{R T_s}, \quad (9)$$

where μ_v and μ_d are the molecular masses of water vapour and dry air, $\mu_v = 0.0180152$ kg mol^{-1} and $\mu_d = 0.028967$ kg mol^{-1}, respectively. R is the molar gas constant. The volume percentage of water vapour in the air is relatively low and ranges from 0% to as high as 4–5%. Subsequently, the partial pressure of dry air dominates.

The partial pressure of water vapour in air is commonly expressed in terms of the relatively humidity,

$$\mathrm{rh} = \frac{p_v}{p_s} 100. \quad (10)$$

The pressure p_s is the saturation pressure of water vapour at the same temperature. It is defined using an approximation for the Clausius–Clapeyron equation

$$p_s(T) = p_{s0}\exp\left[\frac{L}{R_v}\left(\frac{1}{T_0}-\frac{1}{T}\right)\right], \tag{11}$$

where p_{s0} and T_0 are the triple point pressure and temperature. R_v is the gas constant for water vapour.

The water vapour flux is often given by Fick's law

$$J_v = -D\frac{\partial P_v}{\partial z}, \tag{12}$$

where J_v is the water vapour flux and D is the diffusion constant. Theoretically, Fick's law is only valid for isothermal processes and a more general law is required. According to Kestin et al. (1988), the diffusion of a gas in a binary mixture may be given as

$$J_v = -D_e\left(\frac{\partial P_v}{\partial z} - \alpha_{th}\left[\frac{P_v P_d(\mu_v+\mu_d)^2}{(P_v+P_d)\mu_v\mu_d}\frac{1}{T_s}\frac{\partial T_s}{\partial z}\right]\right) \tag{13}$$

where D_e is the diffusion constant for the concentration gradient and $D_e\alpha_{th}$ is the diffusion constant for the thermal gradient. This law has the advantage that when no concentration gradient exists, vapour mass is still transported because of temperature differences. Imposing the conservation of mass on the air phase leads to the differential equation:

$$\theta_a(z,\ t)\frac{\partial(P_v)}{\partial t} + \theta_a(z,\ t)\frac{\partial J_v}{\partial z} = M_{mm}(z,\ t), \tag{14}$$

where M_{mm} is a mass sink or source term due to deposition or sublimation of water vapour onto the ice matrix. It is the mass term which accompanies Q_{mm} in the energy balance equation. Substitution of the thermal flux term leads to

$$\theta_a\frac{\partial P_v}{\partial t} - \theta_a D_e\frac{\partial^2 P_v}{\partial z^2} + \theta_a D_e\frac{\partial}{\partial z} \times\left(\alpha_{th}\left[\frac{P_v P_d(\mu_v+\mu_d)^2}{(P_v+P_d)\mu_v\mu_d}\frac{1}{T_s}\frac{\partial T_s}{\partial z}\right]\right) = M_{mm}. \tag{15}$$

3.3. Water transport equation (mass conservation of water phase)

The water phase mass (volume) conservation equation is written in general terms as

$$\frac{\partial\theta_w}{\partial t} - \frac{\partial J_w}{\partial z} = M_{pc}, \tag{16}$$

where J_w is the rate of water flow per unit area and M_{pc} is a phase change sink our source term (per unit volume) arising from meltwater refreezing or subsurface melting, respectively (Section 6). Often, Darcy's law relating water flow and matrix pressure

$$J_w = D_w\frac{\partial p}{\partial z} \tag{17}$$

is substituted into the above equation to arrive at a diffusion equation. This approach is not adopted here because Darcy's law is not valid for an unsaturated porous medium like snow. The volumetric water content is seldom higher than $\theta_w = 0.15$. The constitutive laws governing unsaturated homogeneous water flow in the snowpack are highly nonlinear, for the most part unknown and require a temporal resolution that is much finer than the energy or settlement equation. They are not computationally tractable for an operational snowpack model. Furthermore, water flow is not homogeneous, rather dominated by so-called preferential flow paths (Schneebeli, 1995). Subsequently, water discharge is modelled poorly using Darcy's law.

For the above reasons, we define the gradient in water flow as

$$\frac{\partial J_w}{\partial z} = 0 \quad \text{for} \quad \theta_w \le \theta_r, \tag{18}$$

$$\frac{\partial J_w}{\partial z} = \dot{\theta}_f \quad \text{for} \quad \theta_w > \theta_r. \tag{19}$$

with

$$\dot{\theta}_f = \frac{\partial(\theta_w-\theta_r)}{\partial t}, \tag{20}$$

where θ_r is the residual water content; that is, below this volumetric content, free water remains fixed within the ice matrix. No transport is possible. Above this value, the excess water is transported immediately

to the adjoining layer at the rate $\dot{\theta}_f$. Presently, a constant value of $\theta_r = 0.08$ is employed in our simulations based on experimental observations (Kattelmann, 1986). As will be shown in the example simulations in Part III, this formulation allows intense melting periods in Spring to be correctly modelled. In the future, θ_r will be a function of snow microstructure.

3.4. Settlement equation (momentum conservation of ice phase)

The settlement equation is:

$$\frac{\partial \sigma_s(z,\ t)}{\partial z} + P_s(z,\ t) g \cos\phi = 0, \tag{21}$$

where σ_s is the stress normal to the slope, g is the gravitational acceleration and ϕ is the slope angle.

A one-dimensional model is statically determinate. In an n layer snowpack, the stress in layer l is given by (layers are numbered from the bottom up)

$$\sigma_s(z) = \left[P_l g(z_l - z) + \sum_{j=l+1}^{n} P_j g(z_j - z_{j-1}) \right] \cos\phi, \tag{22}$$

where P_l is the density of layer l. On an infinite slope of constant slope, the shear stress is defined exactly as

$$\tau_s(z) = \left[P_l g(z_l - z) + \sum_{j=l+1}^{n} P_j g(z_j - z_{j-1}) \right] \sin\phi. \tag{23}$$

Any change of the snowcover in the x- or y-directions (slope changes, different layering) would disturb this stress state. The one-dimensional model represents an idealized, but fully defined, stress state.

Theoretically, it would be possible to break the intrinsic mean stress into different partial stresses, as proposed in mixture theory,

$$\sigma_s = \theta_i \sigma_i + \theta_w \sigma_w + \theta_a \sigma_a. \tag{24}$$

However, there is little practical incentive for doing so since the water and air partial stresses σ_w and σ_a are not of interest. These equilibrium stresses should not be confused with the pore and air matrix pressures, p_w and p_a, which are of great importance for snow metamorphism and water transport. Note that σ_i also differs from the microstructural grain-bond stress, $\sigma_b, \sigma_b > \sigma_i$.

Snow is in a continual state of deformation. Whereas the state of stress is known (in a one-dimensional model), the rate of deformation and the total state of strain are unknown. The deformations are both large and instationary. Snow density (P_s) will increase from <30 to >400 kg/m^3, implying volumetric strains of well over 1000%. In general, the deformations occur at a much faster rate for lower density snow (strains rates $\dot{\epsilon} \approx 10^{-4}$ s^{-1} than higher density snow (strains rates $\dot{\epsilon} \approx 10^{-7}$ s^{-1}).

The complete mathematical description of deformation requires in addition to the single momentum conservation equation: (1) a kinematic description of snow that relates the state of deformation to the total state of strain $\epsilon(z, t)$; (2) a constitutive formulation for Young's modulus that relates the mean stress to the elastic strain, $\epsilon_e(z, t)$ and (3) a constitutive formulation for the viscosity relating the stress to the viscous strain, $\epsilon_v(z, t)$.

A log strain or natural strain measure is employed since it is valid for large strains and deformations (Crisfield, 1991). Given a snow layer with height h_l and original height h_0, the total strain, ϵ, is defined as

$$\epsilon = \int_{h_0}^{h_l} \frac{\mathrm{d}h}{h} = \ln\left(\frac{h_l}{h_0}\right). \tag{25}$$

Bader and Weilenmann (1992) and also Brun et al. (1989) employ a small strain measure. Therefore, the constitutive laws employed in their models cannot be directly used in SNOWPACK.

The total strain is divided into an elastic, ϵ_e, and viscous, ϵ_v, parts,

$$\epsilon = \epsilon_e + \epsilon_v. \tag{26}$$

The viscous strains are large and irreversible and in general $\epsilon_v \gg \epsilon_e$. The constitutive law relates the elastic mean stress to the elastic strain,

$$\sigma_s = E_s \epsilon_e = E_s(\epsilon - \epsilon_v), \tag{27}$$

where E_s is the density- and temperature-dependent bulk modulus of elasticity of snow (see Mellor, 1975).

A simple rheological Maxwell law relates the viscous strain rate, ϵ_v to the mean stress,

$$\dot{\epsilon}_v = \frac{\sigma_s}{\eta_s}, \tag{28}$$

where η_s is the snow viscosity. As shown by Mellor (1975), the viscosity of snow can vary by several orders of magnitude over the density range we are interested in, 50 kg m^{-3} < P_s < 400 kg m^{-3}. Presently, laboratory triaxial tests are underway to determine the viscosity not only as a function of density, but of microstructure as well (Bartelt and Von Moos, 2000). The microstructure-based viscosity formulation will be discussed in Part II of this paper.

An error would be to define snow as a plastic material since the deformations under loading are irreversible. Plasticity theory, however, cannot be applied to model snow behaviour since the two basic tenets of plasticity theory, (1) a time-independent yield surface exists and (2) the direction of plastic flow is defined in some relation to the yield surface (associative or nonassociative flow) have never been experimentally verified. Besides, a viscoelastic material also accounts for nonelastic irreversible deformations. As shown in Bartelt and von Moos (2000), even a simple rheological Maxwell law (Eq. (28)) using a density-dependent viscosity function can accurately model snow behaviour, especially during a loading phase. The law becomes inaccurate during unloading.

4. Initial and boundary conditions

Initial and boundary conditions are an essential part of snowpack modelling.

In SNOWPACK, "initial" implies the specification of a new snowfall mass that occurs within some time interval Δt beginning at time, t_n. The mass is expressed in terms of new snowfall height, Δh_n, and new snowfall density, P_n. The existing height of the snowpack, h, is then updated. The new snowfall height is discretized into finite elements which are added to the existing finite-element grid. The determination of Δh_n and P_n, which is based on measured meteorological data (air temperature and wind speed), is discussed in detail in Part III of this paper. Knowing the density, the volumetric contents, θ, of the new snow can be determined. At present, we usually assume that new snow at high elevations is dry in January and February:

$$\theta_w(t_n,\ z) = 0 \quad \text{for} \quad h \le z \le h + \Delta h_n. \tag{29}$$

Mixed rain/snow events at lower elevations where $\theta_w(t_n,\ z) \neq 0$ are also possible, especially in late Winter and Spring. The initial temperature of the new snow is

$$T(t_n,\ z) = T_n \quad \text{for} \quad h \le z \le h + \Delta h_n. \tag{30}$$

T_n is the air temperature which can change during the course of a snowfall. The initial vapour pressure is determined by assuming that the moist air within the new snow ice lattice is at the fully saturated vapour pressure, p_s, which is a function of the temperature, T_n:

$$p_a(t_n,\ z) = p_s(T_n) \quad \text{for} \quad h \le z \le h + \Delta h_n. \tag{31}$$

Over the snowfall time interval, Δt, new snow falls in an undeformed state,

$$U_i(t_n,\ z) = 0 \quad \text{for} \quad h \le z \le h + \Delta h_n. \tag{32}$$

U_i represents the displacement of the ice matrix. The initial strains are all zero. The initial stress σ_s is easily determined from the overburden pressure. Because new snowfall periods are usually much greater than Δt, new snow mass is introduced into the system over many time intervals. Deformations in the underlying snow layers, therefore, begins instantaneously. Eqs. (29)–(32) define the initial conditions for the four governing differential equations.

Not only do the continuum parameters have to be initialized. The microstructure of the new snow—most importantly the initial grain size—must also be specified. The microstructure of new snow is presented in Part II.

By far, the most important boundary condition governs the energy exchange on the snowpack surface. In SNOWPACK, two possibilities are possible. The first is the usual Neumann boundary condition,

$$k_s \frac{\partial T_s(z = h,\ t)}{\partial z} = q_{lw} + q_{sh} + q_{lh} + q_{rr} \tag{33}$$

where q_{lw} is the net long-wave radiation energy, q_{sh} is the sensible heat exchange, q_{lh} is the latent heat

exchange and q_{rr} is the heat flux from rain. A heat exchange is positive when energy is put into the snowpack; negative when energy is withdrawn. The heat fluxes are discussed in Part III.

The automatic weather stations measure the surface temperature, T_h, directly. Therefore, the second possibility is to specify the Dirichlet boundary condition directly

$$T_s(z=h,\ t)=T_h(t) \tag{34}$$

The Dirichlet boundary condition cannot be used during ablation periods, since the temperature at the snowpack's surface is then always 0 °C. Specifying the Dirichlet condition in this case would underestimate the true energy input. Thus, SNOWPACK employs both conditions. When the surface temperature is well below the melting temperature, the Dirichlet condition is used; when the surface temperature approaches the melting temperature, the program automatically switches to the Neumann condition. At the ground interface, an additional Dirichlet condition is specified,

$$T(z=0,\ t)=T_g(t) \tag{35}$$

where T_g is the measured ground temperature, which does not vary significantly from 0 °C.

The only constraint placed on the settlement equation is that the displacement at the snowpack's base is always zero,

$$U_i(z=0,\ t)=0. \tag{36}$$

Two Neumann boundary conditions are specified for the vapour diffusion equation:

$$D\frac{\partial P_v}{\partial z}=q_h \tag{37}$$

$$D\frac{\partial P_v}{\partial z}=0 \tag{38}$$

where q_h is the vapour mass flux at the snowpack surface. The mass flux is determined by noting that $q_{lw}=Lq_h$. The latent heat flux q_{lw} is discussed in Part III.

5. Numerical solution

The four governing differential equations are solved with the finite-element method. The finite-element approximation leads to the following matrix system

$$[\mathbf{C}]\{\dot{\mathbf{S}}\}+[\mathbf{K}]\{\mathbf{T}\}=\{\mathbf{Q}\} \tag{39}$$

where $\{\mathbf{S}\}^{\mathbf{T}}$ is the vector of unknown field variables,

$$\{\mathbf{S}\}^{\mathbf{T}}=\{\mathbf{T}_s,\ \theta_w,\ \mathbf{u}_i,\ \mathbf{P}_v\}. \tag{40}$$

The unknown variables are defined at the N finite-element nodes. For example, the snow temperatures at the N nodes are $\{\mathbf{T}_s\}^{\mathbf{T}}=\{\mathbf{T}_{s1},\ \mathbf{T}_{s2},\ \ldots,\ \mathbf{T}_{sN}\}$. The matrices $[\mathbf{C}]$ and $[\mathbf{K}]$ and right-hand side vector $\{\mathbf{Q}\}$ are defined according to

$$[\mathbf{C}]=\begin{bmatrix}\mathbf{C}_T & 0 & 0 & 0\\ 0 & \mathbf{C}_w & 0 & 0\\ 0 & 0 & 0 & 0\\ 0 & 0 & 0 & \mathbf{C}_p\end{bmatrix} \tag{41}$$

$$[\mathbf{K}]=\begin{bmatrix}\mathbf{K}_T & 0 & 0 & 0\\ 0 & 0 & 0 & 0\\ 0 & 0 & \mathbf{K}_u & 0\\ 0 & 0 & 0 & \mathbf{K}_p\end{bmatrix} \tag{42}$$

$$\{\mathbf{Q}\}^{\mathbf{T}}=\{\mathbf{Q}_T,\ \mathbf{M}_w,\ \mathbf{F}_u,\ \mathbf{M}_p\} \tag{43}$$

where $[\mathbf{K}_T]$, $[\mathbf{K}_p]$ and $[\mathbf{K}_u]$ are the finite-element heat conductivity, vapour diffusion and stiffness matrices, respectively. The matrices $[\mathbf{C}_T]$, $[\mathbf{C}_p]$ and $[\mathbf{C}_w]$ are the specific heat, water vapour and water capacity matrices, respectively. The right-hand side vector $\{\mathbf{Q}\}$ contains

1. the energy sink or source terms per unit volume per unit time, $\{\mathbf{Q}_T\}$, containing contributions from

short-wave radiation, Q_{sw}, phase changes, Q_{pc} and snow metamorphism, Q_{mm},
2. $\{\mathbf{M}_w\}$, the mass of meltwater produced or refrozen per unit volume per unit time.
3. $\{\mathbf{F}_u\}$, the self-weight of the snowpack and
4. $\{\mathbf{M}_p\}$, the water vapour mass arising from sublimation (positive sign) or deposition (negative sign) of water vapour to and from the ice matrix,

The matrices [**C**] and [**K**] are diagonal and, therefore, the system is only loosely coupled via the constitutive relations and right-hand side vector $\{\mathbf{Q}\}$. For example, phase changes couple $\{\mathbf{Q}_T\}$, the right-hand side of the energy equation containing the latent heat energy of the phase change, as well as $\{\mathbf{M}_w\}$, the mass of water generated or refrozen. Phase changes modify both the volumetric water content θ_w and ice content θ_i and, thus, the finite-element matrices $[\mathbf{K}_T]$ and $[\mathbf{K}_u]$, i.e. the temperature distribution and settlement of the snowpack.

Each equation of the matrix system Eq. (39) is solved independently, using a block Gauss–Seidel method.

6. Melting and refreezing (Q_{pc} and M_{pc})

The link between meteorological energy input, primarily from intense short-wave radiation in the Spring, and surface and subsurface melting is valuable information for both avalanche forecasters and snow hydrologists. In this section, the numerical procedures to model phase changes at the snowpack surface (sublimation, condensation, melting) and snowpack interior (meltwater refreezing, subsurface melting) are explained.

Meltwater refreezing and subsurface melting are treated at the finite-element level as volumetric heat sources and sinks, respectively, that correspond to changes in an element's volumetric ice and water contents. The procedure is mass conserving. In this section, we describe only the generation of meltwater and do not discuss the transport of water across element boundaries.

Subsurface melting is treated as a constraint on the temperature field: the temperature $T_s(z, t)$, can never be greater than 0 °C. Even if the numerical heat transfer solution produces temperatures which are $T_s(z, t)>0°$, say from intense short-wave radiation, the snow temperature must remain at $T_s(z, t)=0°$. The "excess" energy is used to drive the melting process. Moreover, the energy input is used to melt the ice matrix, and not to raise the temperature of the snowpack to some unphysical value.

Let ΔT be the difference between the calculated snow temperature T_s' and the melting temperature, $T_m=0$ °C,

$$\Delta T = T_s' - T_m. \tag{44}$$

For melting to occur, $T_s' > T_m$ or $\Delta T>0$ °C. The mass of meltwater Δm_w that can be produced is

$$\Delta m_w = \frac{c_i m_i \Delta T_s}{L_f} \tag{45}$$

where $L_f=334{,}000$ J kg^{-1} is the latent heat of fusion, c_i is the specific heat of ice, m_i is the ice mass. Since the volumetric ice and water contents are used throughout the computations to describe the snow matrix, the above equation can also be written,

$$\Delta\theta_w = \frac{c_i \theta_i P_i \Delta T_s}{L_f P_w} \tag{46}$$

Since mass is at all times conserved, $\Delta m_w = -\Delta m_i$. The change in volumetric ice content is then

$$\Delta\theta_i = \frac{P_w \Delta\theta_w}{P_i}. \tag{47}$$

The latent heat energy per unit volume required for the phase change is

$$Q_{pc} = L_f \Delta\theta_i P_i. \tag{48}$$

Note that in the case of melting $\Delta\theta_i$ is negative and Q_{pc} is consequently a heat sink. This term is added to the governing differential energy equation at the next time step to enforce the $T_s(z, t)=T_m$ temperature constraint.

Meltwater refreezing is treated similarly to subsurface melting. For meltwater refreezing to occur, two conditions are required. Firstly, meltwater is present ($\theta_w>0$) and secondly the calculated temperature of the snow, $T_s(z, t)$, is below 0 °C. Since the temperature of

the meltwater is always assumed to be $T_w = 0$ °C (which is also the bulk temperature), the temperature difference between the water and ice phases is

$$\Delta T = T_s - T_w. \tag{49}$$

Unlike the subsurface melting case, in the refreezing case ΔT is negative. The changes in volumetric contents are likewise given by Eqs. (46) and (47). The heat energy released during refreezing is also given by Eq. (48). This time, however, $\Delta\theta_i$ is positive and Q_{pc} is a heat source that raises the bulk temperature of the snowpack.

An important assumption of the algorithm is that the phase change occurs during the time step Δt, that is, the temperature difference ΔT is constant over the entire time step. Depending on the energy input, this might be a poor approximation. The time step length will certainly influence the model results. Typical time steps lengths are 15 min.

Phase changes do not directly alter the stress state of the snowpack. However, since the viscosity and heat conduction are both functions of the volumetric ice and water contents (as well as the snow microstructure), phase changes will directly influence the settlement velocities.

7. Mass and energy exchanges due to interlayer diffusion (Q_{mm} and M_{mm})

For any given temperature, the calculated vapour pressure cannot be greater than the saturation pressure. Similar to the case discussed in the previous section, where the melting temperature is a constraint on the temperature field, the saturation pressure is a constraint on the vapour pressure field, p_v. Mass and energy exchanges are derived that impose this condition.

The difference between the calculated vapour pressure (p'_v) and saturation pressure is given by,

$$\Delta p = p'_v - p_s. \tag{50}$$

The excess mass of vapour in the pore air (Δm_v) that must be deposited on the ice lattice (Δm_i) to enforce the saturation constraint is

$$\Delta m_v = -\Delta m_i = -\frac{V_a \mu_v}{RT_s}\Delta p. \tag{51}$$

The change per unit volume over the time step Δt is

$$M_{mm} = \frac{\Delta m_v}{V_a \Delta t} = -\frac{\theta_a \mu_v}{RT_s}\frac{\Delta p}{\Delta t}. \tag{52}$$

The associated energy exchange is

$$Q_{mm} = L_s M_{mm}. \tag{53}$$

For the case when the $p_v < p_s$ (undersaturated), $M_{mm} = Q_{mm} = 0$. The change in volumetric ice content is

$$\Delta\theta_i = \frac{\theta_a \mu_v}{P_i RT_s}\Delta p. \tag{54}$$

8. Comparison between simulation and measurement

8.1. Simulation of the catastrophic avalanche winter 1999

The catastrophic avalanche winter of 1999 will be used to demonstrate the main features of SNOWPACK. The purpose of this section is to provide a general overview of the program: input, calculation results, calculation times and output features.

The winter of 1999 was highlighted by three extreme snowfall periods that occurred in late January and February. The development of the snowpack at SLF's field test site is shown in Fig. 2. This figure depicts the microstructural development of the snowpack from dendritic new snow grains (shown in green and denoted with the symbol ++) to melt forms (red and denoted with ○○). Faceted crystal layers are shown in blue. Layers of buried surface hoar are also depicted.

The diagram depicts some general results that agree with observations. For example, the layers of faceted crystals at the base of the snowpack or the time it takes to break down the dendritic structure of the new snow. Note also the change of the crystals to melt–freeze types in Spring.

The calculated and measured snow heights are compared in Fig. 3 and are in good agreement.

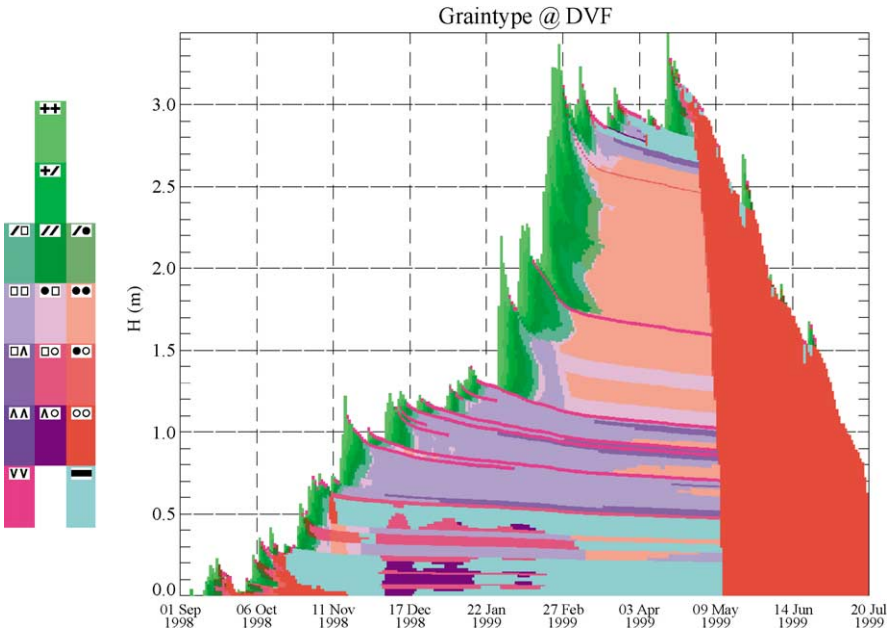

Fig. 2. The microstructural development of the snowpack during the catastrophic avalanche winter 1999. The colour green depicts new snow which changes to well-rounded grains (red) or faceted grains (blue).

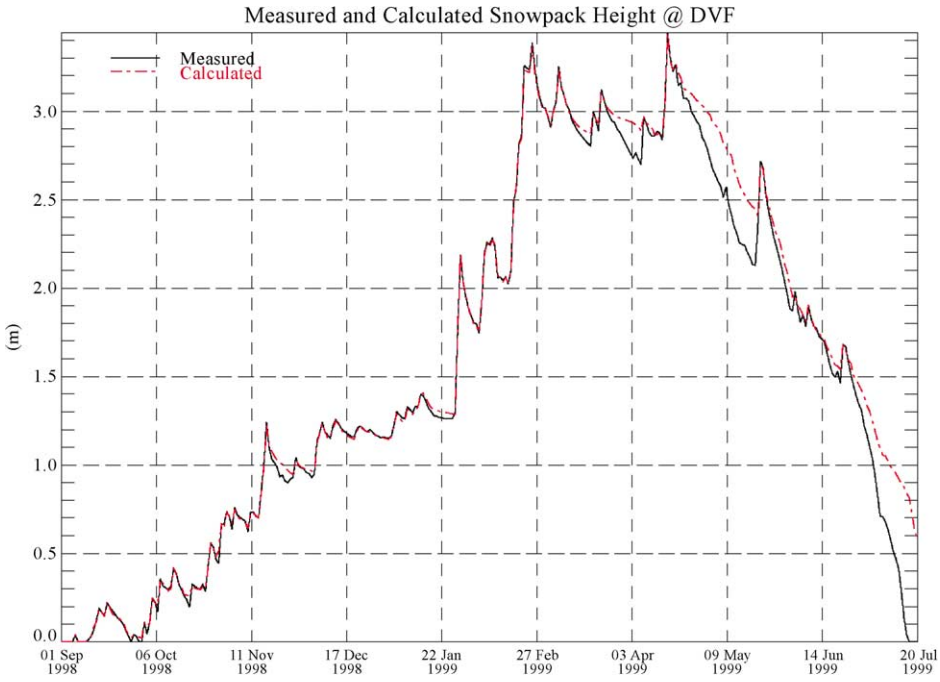

Fig. 3. Calculated and measured snowpack heights.

However, this result is misleading, since the measured snow heights are being used to drive the new snowfall amounts. As soon as the measured and calculated heights are not in agreement, then new snow is added (finite elements are added to the existing grid). This procedure will not work if the snowpack settles too quickly; that is, when the snowpack layers densify too quickly. In this case, too much mass will be added to the snowpack. Therefore, not only must the calculated snow heights agree with measurements, but also the density of the snow layers. The density of the snowpack is shown in Fig. 4.

Note that the densities (P) range between 30 and 400 kg m^{-3}, with the higher densities occurring during the Spring melt period. Note a generally good agreement between measured and calculated snow heights with the exception of a small systematic underestimation of snow ablation.

The physical parameter which controls the densification of the snowpack is the viscosity. The elastic deformations are small. Irreversible viscous strains can be very large, sometimes as high as 500%. As shown in Fig. 5, the viscosity will range over several orders of magnitude over the course of the winter. Note the change in viscosity as the grains change form and during the Spring melting period.

It is important to emphasize the highly nonlinear, complex and fragile interaction between the temperature and settlement fields. The viscosity is a function of the layer microstructure (see Part II) which is determined by the thermal regime of the snowpack (temperature and temperature gradient). The thermal regime is primarily a function of the surface energy exchanges and heat conductivity. The heat conductivity, however, is not only dependent on the microstructure but also on the density—the settlement of the snowcover. Thus, the fields are strongly coupled and if one field provides erroneous results—either the temperature or settlement—then the calculated values will immediately depart from the real solution.

The temperature in the snowpack over the entire winter is depicted in Fig. 6. Recall that the temperature field is being constrained by two Dirichlet boundary conditions—the measured ground and surface temperatures—as long as the temperatures remain under -1.3 °C. As soon as the surface temperature approaches the melting temperature, then

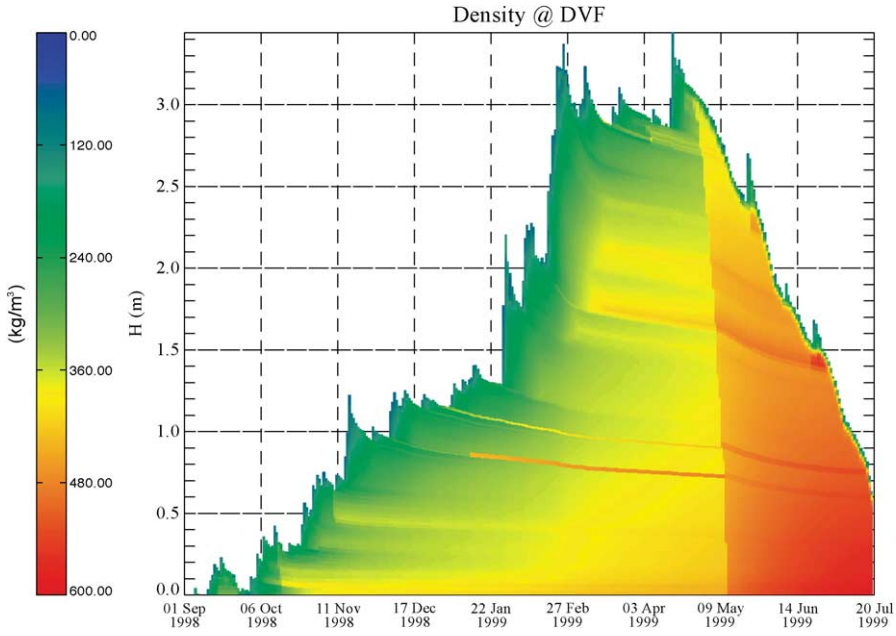

Fig. 4. Snowpack density during the winter of 1999.

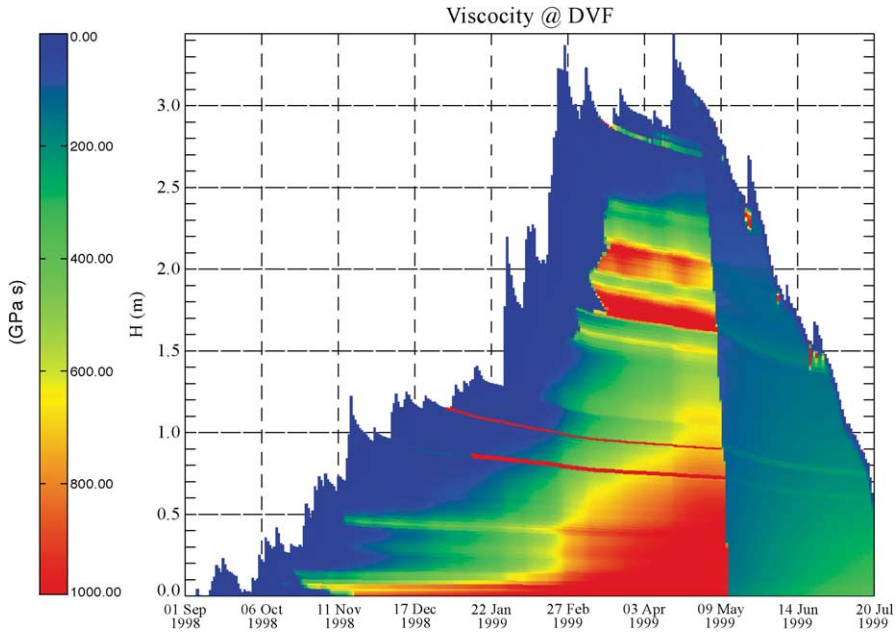

Fig. 5. Viscosity.

the surface boundary condition changes to a Neumann condition, in order to calculate the heat fluxes which are driving the surface melting.

The automatic weather stations measure snowpack temperatures at 25-, 50- and 100-cm depths (measured from the bottom) continuously. This data

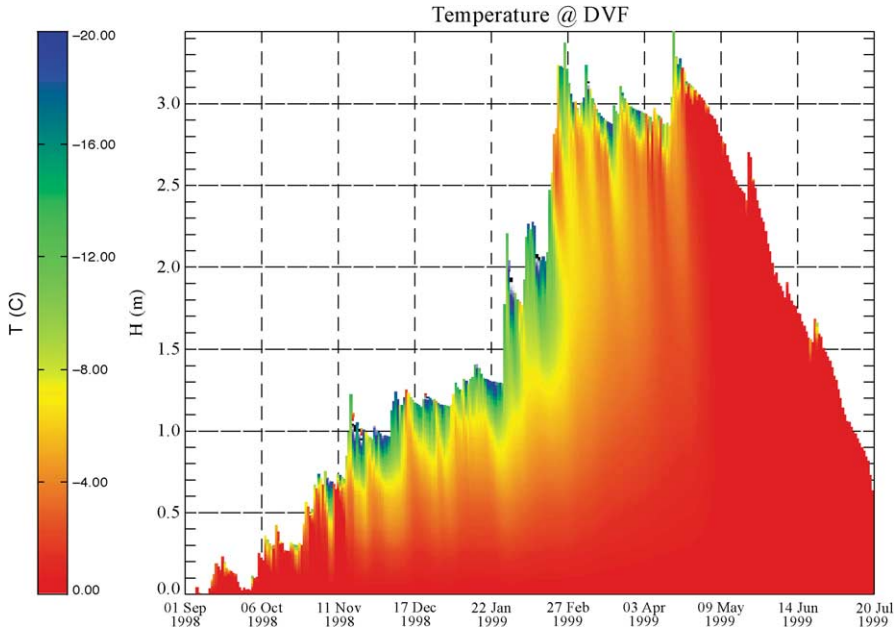

Fig. 6. Temperature.

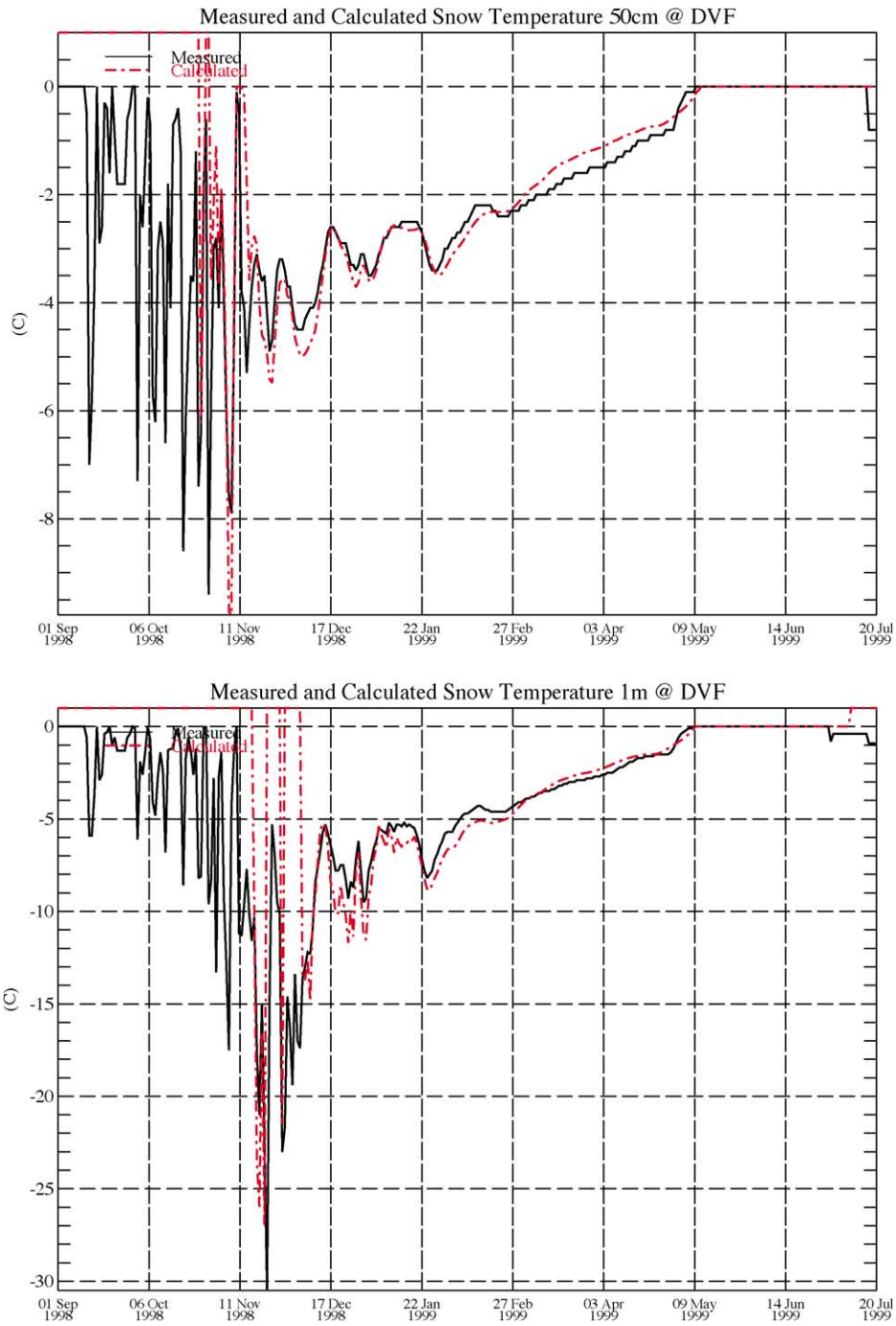

Fig. 7. Measured and calculated snowpack temperatures at 50 and 100 cm above ground. The measured oscillations at the beginning of the winter are due to the fact that the temperature probe is in the air.

is not used to drive the model (as the measured surface temperature), rather to validate the thermal calculations. Specifically, the microstructure based heat conductivity model. Fig. 7 presents a comparison between the measured and calculated temperatures at 50 and 100 cm. The oscillations at the beginning of the comparison are due to the fact that the probes are measuring air temperature because the snowpack has not covered them yet. Note that the model correctly predicts the temperature variations in the snowcover during the Winter and the onset of isothermal conditions.

The volumetric water content is shown in Fig. 8. This diagram shows clearly the isothermal snowpack in April–June. It also shows that the model predicted two small melt periods in mid-November, where the meltwater eventually refroze on the ice lattice. Another melt/refreezing period occurred in the middle of March. Both these events agree with observations. For more detailed evaluations, see Part III.

Of special interest are the two new snowfall periods that occurred in late April and May. These snowfalls deposited nearly 50 cm of fresh snow but began to settle and melt almost immediately. Note also that new snow was deposited in September, but this snow melted entirely. This event demonstrates the practical importance of running the model when no or very few finite elements exist. In this case, the model is awaiting the next new snowfall event. The snowpack in October also underwent a melting phase. The model predicts that free water stayed in the lower depths of the snowpack until beginning of November, when the temperatures cooled significantly.

An important application of snowpack modelling is to predict cumulative water runoff, shown in Fig. 9. This graph shows some runoff in September, followed by a period of no runoff for the high winter snowpack and the subsequent melting period which began around the 5th of May 1999.

8.2. Mass balance check

It is beyond the scope of this paper to evaluate the individual model components. However, we want to assess the overall performance. This is best accomplished by evaluating the mass balance of the seasonal snow pack because the snow mass balance depends not only on the dry snow mass balance (snow fall, wind drift), but also on the energy balance (melting, sublimation, rain).

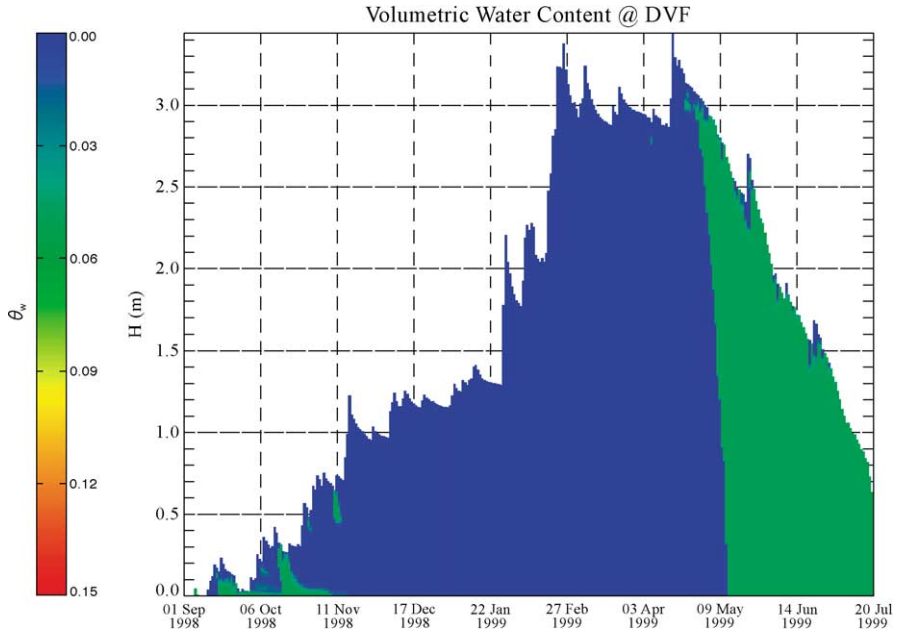

Fig. 8. Volumetric water content.

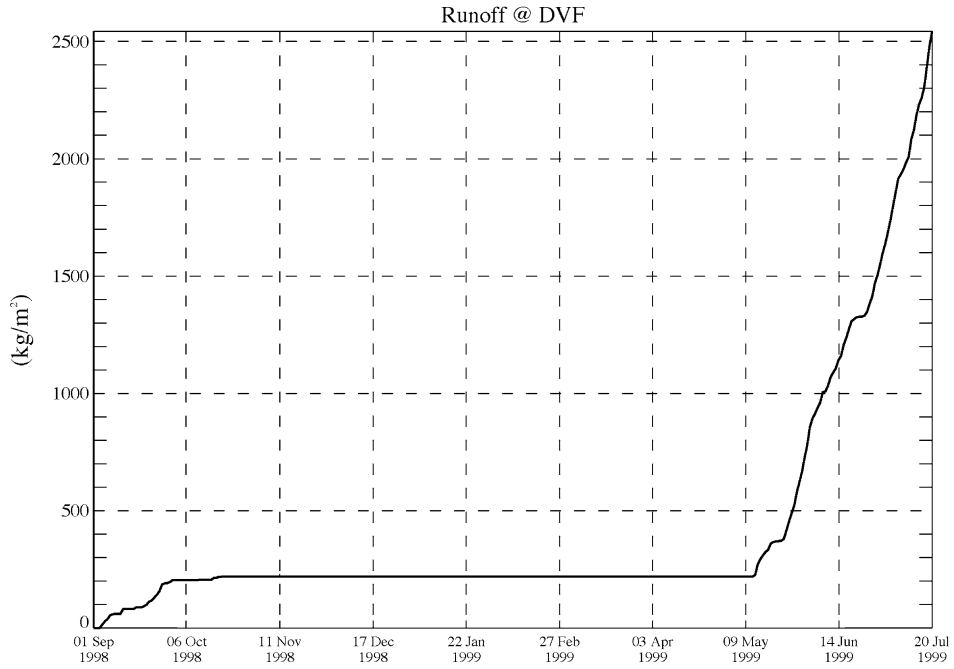

Fig. 9. Cumulative water runoff.

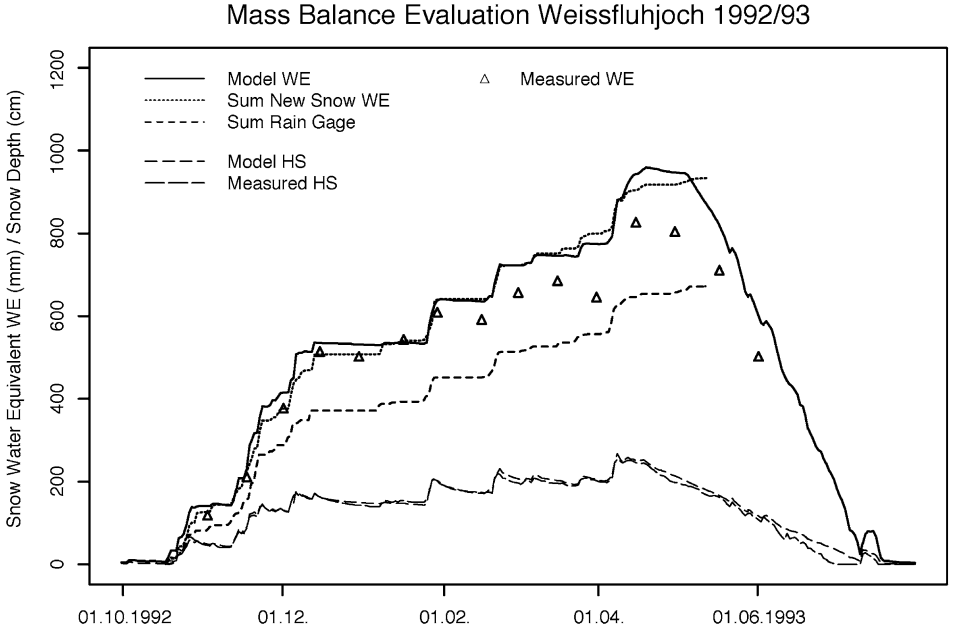

Fig. 10. Mass balance winter 1992/1993.

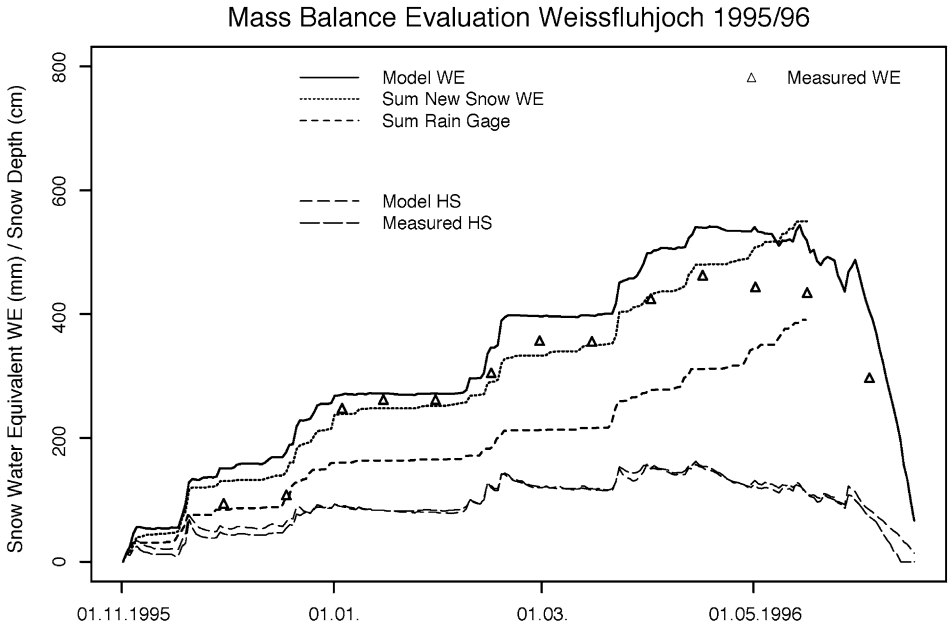

Fig. 11. Mass balance winter 1995/1996.

The Versuchsfeld Weissfluhjoch experimental site is a very well-equipped high Alpine measurement station where a wealth of snow and weather data are collected. We present the evaluation of the overall mass balance for 5 years. These evaluations extend and supplement the evaluations presented in

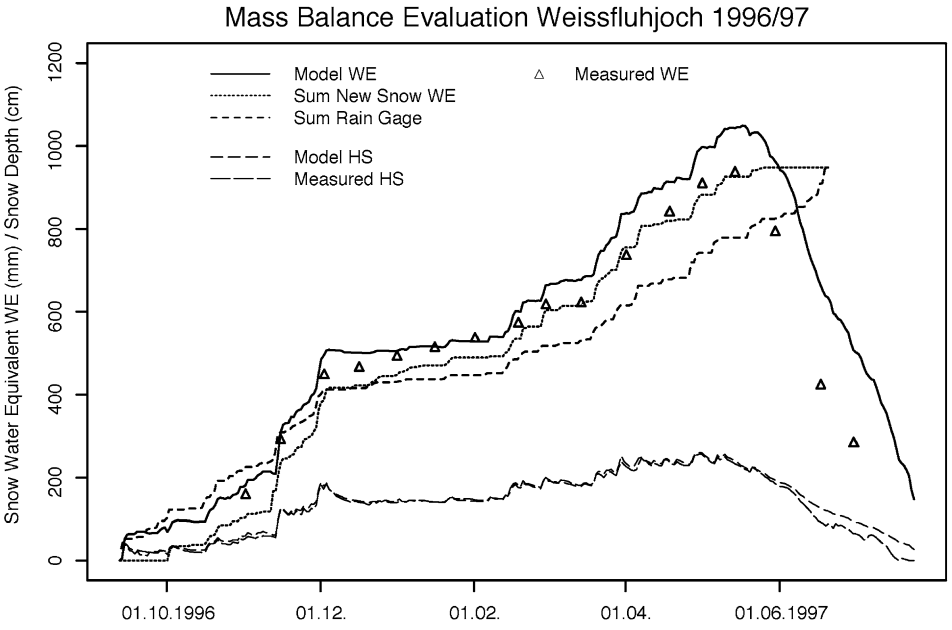

Fig. 12. Mass balance winter 1996/1997.

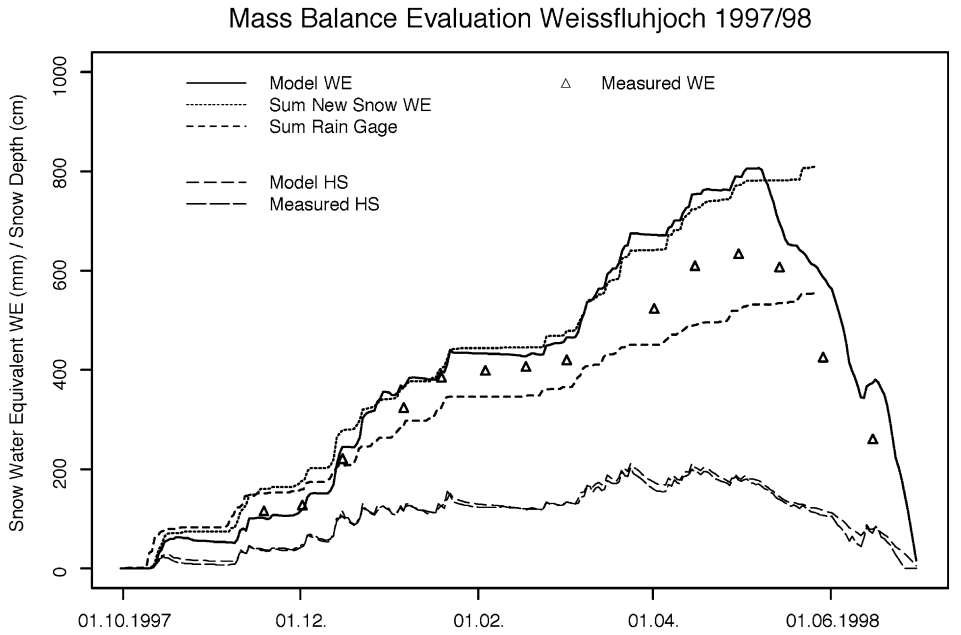

Fig. 13. Mass balance winter 1997/1998.

Lehning et al. (1999) and are also done with a much more recent version of the model. Figs. 10–14 summarize the mass balance results. Shown are the total water equivalent of the snowcover as calculated by the model (Model Water Equivalent—MWE), the sum of the manually measured,

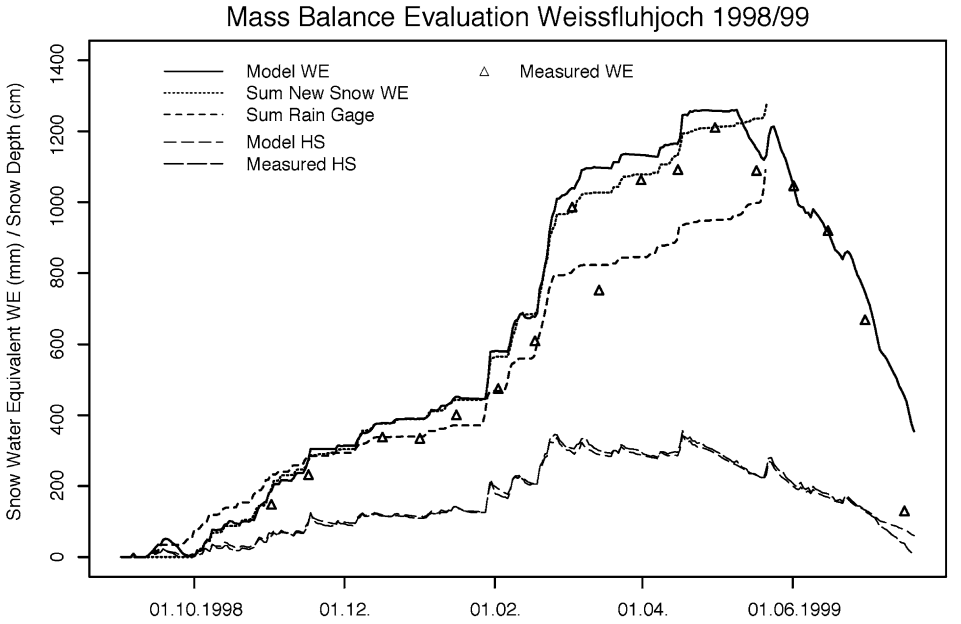

Fig. 14. Mass balance winter 1998/1999.

daily new snow water equivalents (Sum Hand Water Equivalent—SHWE), the manually measured (twice per month) total water equivalent (Hand Total Water Equivalent—HTWE) and the sum of the official weather service rain gage (Sum Rain Gage—SRG). Also shown is a comparison between measured and modelled snow depth.

In agreement with our field experts (SLF, personal communication), we consider SHWE as the best reference up to the yearly maximum snow depth. HTWE is less reliable because the measurements are done during the snow profile assessment, which requires that every profile is done at a new location, moving away from the place of the automatic meteorological measurements during the course of the winter. This judgement is partly based on the inspection of the time series of HTWE, which shows a significant scatter, e.g. the considerable decrease of water equivalent on April 1 in Fig. 10. Since the snowcover is usually completely dry at Weissfluhjoch until the end of March, the only two processes responsible for a possible discrepancy between SHWE and HTWE during the accumulation period would be wind erosion or sublimation. Wind erosion is not of significance at this site and even very high assumed sublimation rates can not explain the observed disagreement. In addition, the disagreement is different from year to year, being largest in 1997/1998 (Fig. 13) and being very small in 1998/1999.

For the different years with a range of the maximum total water equivalent from 540 (Fig. 11) to 1260 mm (Fig. 14), MWE agrees very well with SHWE for the accumulation period. A small systematic overestimation of MWE exists, which is more pronounced in 1995/1996 and 1996/1997. This small overestimation has to be compared to the known snow fall underestimation from the rain gage, which can be very severe (Figs. 10 and 12) at those high Alpine sites. In general, also the melt period is well captured by the model. As can be seen from the snow depth comparison, a systematic underestimation of the melt rate exists during the final stage of the melt season. In summary, the overall mass and energy balance appears to be correctly modelled by SNOWPACK in its operational version, where only measured snow heights are used to determine snow precipitation.

9. Conclusions and outlook

The SNOWPACK software has been applied for the three winters 1998/1999, 1999/2000 and 2000/2001 in now-casting model to predict snowpack settlement and stratigraphy. The model is embedded in an operational system containing automatic weather stations, databases and network visualization software (INFOBOX). The model is front-ended by an automatic system that checks the integrity of the incoming measurements. Calculations are performed for eighty alpine locations. The model results are sent to a central data bank where they can be accessed by avalanche professionals at remote locations throughout the Swiss alps.

During the designing of SNOWPACK, special attention was placed on choosing numerical procedures that allow a more accurate and rational description of snow. These include:

1. A Lagrangian coordinate system to model history-dependent material behaviour (microstructure). The location of the top snowpack surface is known at all time. Layers—discontinuities in density—are accounted for.
2. A multicomponent description (ice, vapour, water) of snow that allows for mass and energy conserving phase changes between components.
3. A large strain description of deformation that accounts for large volumetric deformations of new snow.
4. Highly nonlinear and time-dependent thermal boundary conditions based on meteorological measurements.
5. The addition of finite elements to account for new snow; elimination of elements to account for surface melting.
6. The transport and refreezing of meltwater in the snowpack.
7. Constitutive laws for heat conductivity and viscosity based on grain microstructure.

The finite-element model sequentially solves four differential equations governing the bulk temperature, displacement, water content and vapour concentration in the pore air. The finite-element solution automatically ensures the conservation of the ice mass.

The solution schemes are stable; typical time steps for the implicit time integration are on the order of 15 min. These are based on the fact that meteorological data (air temperature, surface temperature, radiation, wind speed) are measured at 30-min intervals. In addition, new snow settling can be accurately modelled with this time step.

Additional equations governing the energy and momentum balance for the air and water phases could be introduced to create a "full" mixture theory model. This would allow, for example, different temperatures in the air and ice phases to be simulated. However, this also requires that energy and momentum exchanges between the phases be defined. This level of detail might be required in future when simulating laboratory experiments and advancing microstructure theories. Presently, however, we believe it is not required in an operational model, especially since it would increase the computational demands of the model.

One of the clear disadvantages of numerical calculations is that a tremendous amount of data is created that must be easily visualized. The modelling data is not easy for avalanche forecasters who are not familiar with the finite-element method. For this reason, rules that attempt to describe the bulk state of the snowpack are under development. An example is a stability index. This work is similar to the French MEPRA program (Brun et al., 1992). But before a stability index can be formulated, intensive validation studies of the snow layering (density and microstructure) and surface energy balance are required as a first step. This step will be discussed in the second and third parts of the paper. The validation of a stability index will take many years since the relation between avalanche activity and snowpack layering with regards to mechanical strength must be derived from field and laboratory studies.

The SNOWPACK program is now being applied to study ecological and hydrological problems involving the snowcover. An example is to find the difference between natural and artificial snowcovers on the thermal regime of the ground vegetation layer. Ecologists want to study the environmental consequences of using snow canons to prepare ski runs. Another example is to investigate the influence of the snowcover properties on permafrost ground. It is feared that the melting of ice in the permafrost layer will weaken the foundations of many avalanche defense structures. Here, too, model calculations are being performed (Phillips et al., 2000).

Many problems in snow science are not one-dimensional. For example, avalanche formation involves shear forces on weak layers that must be treated with two- or three-dimensional snowpack models. Several modules of SNOWPACK have been directly implemented into a two-dimensional snowpack program called HAEFELI (Bartelt and Christen, 2000). This program was primarily designed to determine the creep forces exerted on avalanche defense structures. It employs the same metamorphism and phase-change routines. Furthermore, the one-dimensional constitutive laws have been extended to two dimensions. The energy exchange at the snowpack surface is modelled using the same convective and radiative boundary conditions. Finally, three-dimensional snowpack models, which simulate the creep and glide movements in complex alpine terrain, are now being projected. It is our plan to model the full three-dimensional stress and deformation state of the snowpack. However, in order to reduce computations, the snowpack layering, microstructure and temperature distribution will be based on one-dimensional SNOWPACK calculations.

Acknowledgements

The authors thank W. Ammann, Head, Swiss Snow and Avalanche Research, for his support during the course of the model development, including the financial support of B. Brown during his stay in Davos. Much of the experimental work was financed by the Swiss National Science Foundation. The authors also wish to thank the avalanche science group at Montana State University—E. Adams, J. Dent, C. Lundy and K. Birkland—for their interest and support in this work.

References

Bader, H.P., Weilenmann, P., 1992. Modeling temperature distribution, energy and mass flow in a (phase-changing) snowpack: I. Model and case studies. Cold Reg. Sci. Technol. 20, 157–181.
Bartelt, P., M. Christen, M., 2000. A computational procedure for

instationary temperature dependent snow creep. In: Hutter, K., Wang, Y., Beer, H. (Eds.), Advances in Cold Region Thermal Engineering and Sciences: Technological, Environmental and Climatological Impact. Proceedings of the 6th International Symposium, Darmstadt, Germany, 22–25 August 1999. Springer-Verlag, Berlin, pp. 367–386, Lecture notes in physics, volume 533.

Bartelt, P., von Moos, M., 2000. Triaxial tests to determine a microstructure-based snow viscosity law. Ann. Glaciol. 31, 457–462.

Brun, E., Martin, E., Simon, V., Gendre, C., Coleou, C., 1989. An energy and mass model of snowcover suitable for operational avalanche forecasting. J. Glaciol. 35, 333–342.

Brun, E., David, P., Sudul, M., Brugnot, G., 1992. A numerical model to simulate snowcover stratigraphy for operational avalanche forecasting. J. Glaciol. 38, 13–22.

Crisfield, M.A., 1991. Non-linear Finite Element Analysis of Solids and Structures: Volume 1. Essentials. Wiley, Chichester, England.

Gray, J.M., Morland, L., 1994. A dry snow pack model. Cold Reg. Sci. Technol. 22, 135–148.

Gray, J.M., Morland, L., 1995. The compaction of polar snow packs. Cold Reg. Sci. Technol. 23, 109–119.

Gray, J.M., Morland, L., Morris, E., 1995. A phase changing dry snowpack model. J. Glaciol. 41 (137), 11–29.

Gubler, H., 1978. Determination of the mean number of bonds per snow grain and of the dependence of the tensile strength of snow on stereological parameters. J. Glaciol. 20 (83), 329–341.

Hansen, A., Brown, R., 1987. A new constitutive theory for snow. Proceedings of the Davos Symposium, September 1986. International Association of Hydrological Sciences Publication, vol. 162, 87–104.

Jordan, R., 1991. A one-dimensional temperature model for a snowcover. CRREL Spec. Rep. 91–16.

Kattelmann, R.C., 1986. Measurements of snow layer water retention. Cold Region Hydrology Symposium, July 1986. American Water Resources Association, pp. 377–386.

Kestin, J., Wakeham, W., Ho, C., 1988. Transport properties of fluids: thermal conductivity, viscosity and diffusion coefficient. The Center for Information and Numerical Data Analysis and Synthesis, Data Series on Material Properties, Group I: Theory, Estimation and Measurement of Properties I-1. Hemisphere Publishing, New York, 344 pp.

Kry, P.R., 1975. The relationship between the visco-elastic and structural properties of fine-grained snow. J. Glaciol. 14 (72), 479–500.

Lehning, M., Bartelt, P., Brown, B., Russi, T., Stoeckli, U., Zimmerli, M., 1999. SNOWPACK model calculations for avalanche warning based upon a new network of weather and snow stations. Cold Reg. Sci. Technol. 30, 145–157.

Lehning, M., Bartelt, P., Brown, B., Fierz, C., Satyawali, P., 2002a. A physical SNOWPACK model for the Swiss avalanche warning: Part II. Snow Microstructure. Cold Reg. Sci. Technol. 35, 147–167

Lehning, M., Bartelt, P., Brown, B., Fierz, C., 2002b. A physical SNOWPACK model for the Swiss avalanche warning: Part III. Meteorological forcing, thin layer formation and evaluation. Cold Reg. Sci. Technol. 35, 169–184

Mahajan, P., Brown, R., 1993. A microstructure-based constitutive law for snow. Ann. Glaciol. 18, 287–294.

Mellor, M., 1975. A review of basic snow mechanics. Snow Mechanics Symposium (Proceedings of the Grindelwald Symposium), April 1974. International Association of Hydrological Sciences Publication, vol. 114, 251–291.

Morland, L.W., Kelly, R.J., Morris, E.M., 1990. A mixture theory for a phase-changing snowpack. Cold Reg. Sci. Technol. 17, 271–285.

Phillips, M., Bartelt, P., Christen, M., 2000. Influences of avalanche-defence snow-supporting structures on ground temperature in Alpine permafrost terrain. Ann. Glaciol. 31, 422–426.

Schneebeli, M., 1995. Development and stability of preferential flow paths in a layered snowpack. IAHS Publ. 228, 89–95.

Swiss Federal Institute for Snow and Avalanche Research (SFISAR), 2000. Der Lawinenwinter 1999. Ereignisanalyse. Eidg. Institut fuer Schnee und Lawinenforschung, Davos.

St. Lawrence, W., Bradley, C., 1975. The deformation of snow in terms of a structural mechanism. Snow Mechanics Symposium (Proceedings of the Grindelwald Symposium), April 1974. International Association of Hydrological Sciences Publication, vol. 114, 155–170.